

Bayesian analysis of low latency LIGO alerts

Nicholas-Tyler Howard¹

September 2021

ABSTRACT

LIGO (Laser Interferometer Gravitational wave Observatory) detectors are capable of detecting gravitational waves created by merging massive stellar remnants moving at high accelerations. Collisions of massive stellar remnants create electromagnetic waves that can reveal many aspects of the remnants that collided. The EM community is attempting to use data from the LIGO instruments to pinpoint the location of the sources and view the sources across all electromagnetic wavelengths as shown by observational campaigns conducted during LIGO’s third observing run. Gravitational wave detectors are poor at localizing mergers, making the discovery of counterparts a challenging task. We will compare the Bayes factor and the Terrestrial probability of alerts as metrics of classifying sources as astrophysical in low latency. We will improve the low latency data products that are provided to EM observers in order to aid in the discovery more counterparts in the future.

1 INTRODUCTION

1.1 Gravitational Waves

Gravitational waves (GWs) are disturbances in space-time caused by an accelerated mass, that propagate away from their source at the speed of light. Because GWs are the result of a pair of massive objects in a decaying orbit around a shared center of mass, their observed signal strength increases as the objects approach one another.

Laser Interferometer Gravitational wave Observatory(LIGO) is an instrument used to observe said propagations in space-time from massive merging stellar remnants. For now, the gravitational waves that LIGO detects are a result of three types of stellar remnant mergers, Binary Black Hole merger(BBH), Binary Neutron Star merger(BNS), and Neutron Star - Black Hole merger(NS-BH).

1.2 LIGO Detectors

LIGO detectors are Michaelson Interferometers (LIGO Scientific Collaboration et al. 2015). The detector consists of one laser, a power and signal recycling mirror, a photon collector, a beam splitter and many other components as shown in fig(1).

The beam splitter splits the beam of light from the laser into two beams of light orthogonal to each other, but the two beams remain parallel to the surface of Earth. The two light beams split from the beam splitter oscillate approximately 300 times individually between mirrors that are separated by 4km for each arm; this distance is equivalent to 1200km.

1.3 Detecting Sources

LIGO detectors aim to detect these disturbances using its powerful laser (750KWatt) and effective length (1200km)(LIGO Scientific Collaboration et al. 2015). When

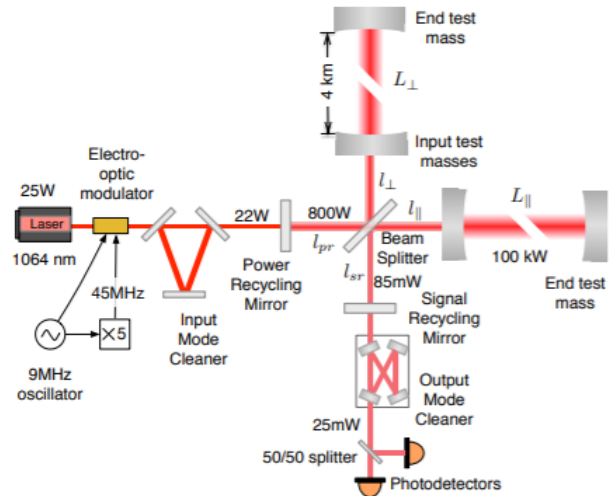


Figure 1. The design for Advanced LIGO detectors from (Martynov et al. 2016)

both beams of light in the arms of LIGO reaches a length of 1200km the beams transmit through the mirrors and interfere destructively with one another. If powerful enough GWs happen to pass through Earth the arms will no longer be the same length which causes a phase difference between the light beams, resulting in the beams not interfering destructively. The photon collector can be used to find the intensity of the GW that causes the strain on the detector.

1.4 Classifying Sources

When LIGO detects a GW, we infer properties of the merger based on the observed signal. After sources are obtained, the

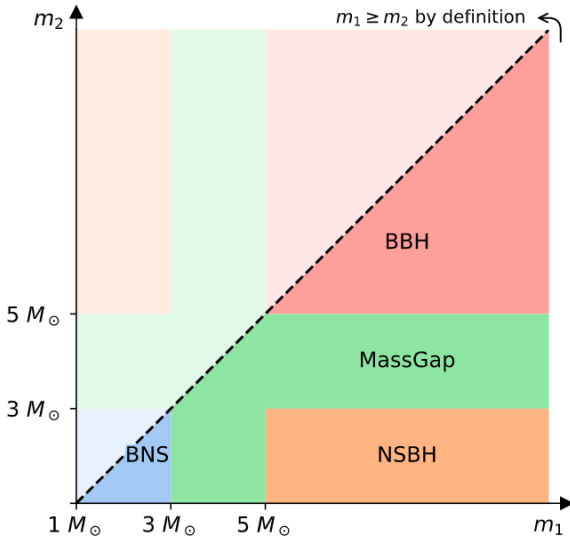


Figure 2. Mass relationship used to classify mergers detected by LIGO where $m_1 \geq m_2$ is always true. This figure defines how pastro is found for alerts. (LIGO Scientific Collaboration 2021)

FAR (False Alarm Rate) is used to determine if the source is astrophysical or not. If the alert passes the FAR threshold, we then analyze the signal to determine what two objects collided to create the GW. From the strain caused by a GW on the LIGO lasers, one can directly determine the chirp mass. This parameter is derived from the masses of the two merging astronomical objects.

The chirp mass is defined as (Chen & Shen 2019):

$$M = \frac{(m_1 m_2)^{3/5}}{(m_1 + m_2)^{1/5}} \quad (\text{Kapadia et al. 2020}) \quad (1)$$

M is the chirp mass with m_1 and m_2 being the mass of the two objects. The chirp mass allows us to use the mass from sources to classify them depending on their mass.¹

As shown in fig(2) the ratio of mass between the two colliding objects reveals the types of objects that collided. There are five classifications for sources.

BNS Mergers consist of a Binary Neutron Star (BNS) system, as shown on fig(2) they are relatively low in mass, with masses between 1-3 solar masses²

A NSBH merger consists of a Black Hole and a Neutron Star colliding with one another. These collisions are classified from mid-sized mass detections that are greater than 5 Solar Masses for the most massive object and between 1-3 solar masses for the less massive object.

BBH³ mergers consist of two black holes colliding. These collisions are typically between two massive objects. Both the low mass and high mass object have masses that are greater than 5 Solar Masses.

MassGap mergers consist of at least one intermediate mass object with a mass in a range of 3-5 solar masses. When an object is in this mass range we are unsure of what to label it.

¹ LIGO is most sensitive to a combination of ≈ 10 solar masses

² A Solar Mass is the mass of the sun

³ Binary Black Hole

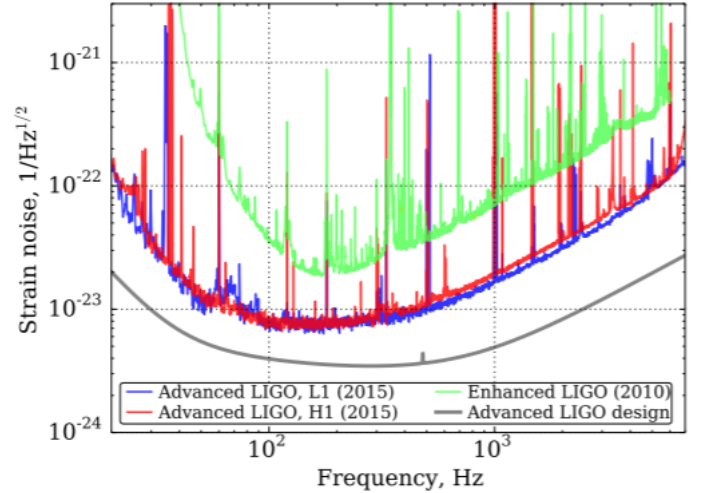


Figure 3. The gray curve is the amplitude spectral density for the Advanced LIGO detector, it is the design sensitivity for advanced LIGO. This figure shows the strain noise as a function of frequency in the detectors. All of this noise must be reduced for LIGO to detect gravitational waves. (Martynov et al. 2016)

Finally we have the classification of Terrestrial events. If a detection is classified as Terrestrial, it is not astrophysical. Terrestrial signals could be a result of the noise artifacts in the LIGO instrument or disturbance from the environment near the instrument.

1.5 Validity of Sources

The process explained in the previous sections, in practice, is difficult, as any disturbance to the mirrors will result in the photon collector collecting light. To counter this a considerable amount of noise must be filtered out of the detectors. The LIGO detector itself will generate noise; to counter this we search for GW waves in frequencies where the detector does not generate a substantial amount of noise.

The False Alarm Rate (FAR) is used to determine if a detected source is astrophysical or not. FAR is defined as:

$$FAR(\rho) = \int_{\rho}^{\rho_{max}} \Lambda_n p_n(\rho') (d\rho') \quad (2)$$

Where ρ is the SNR (Signal to Noise Ratio), Λ_n is the mean Poisson rate of signal and noise triggers (Callister et al. 2017), p_n is the probability density describing the distribution of detection statistics of ρ . The False Alarm Rate (FAR) is equal to 10^{-2} per year and is the current method used to check if an object is astrophysical source (Callister et al. 2017).

1.6 Bayesian Statistics

$$P(H_i | \vec{d}, I) = \frac{P(H_i | I) P(\vec{d} | H_i, I)}{P(\vec{d} | I)} \quad (3)$$

Bayesian inference, the probability of a hypothesis H_i when given a set of observational data \vec{d} and prior information I

is given by eqn(3). $P(H_i|I)$ is the prior probability of H_i , $P(d|H_i, I)$ is the likelihood function of the data, given that H_i is true and:

$$P(\vec{d}|I) = \sum P(\vec{d}|H_i, I) \quad (4)$$

eqn(4) is the minimum probability of the data set d . We can compare models by calculating probabilities in the form of “posterior odds ratio”:

$$O_{ij} = \frac{P(H_i|I)P(\vec{d}|H_i, I)}{P(H_j|I)P(\vec{d}|H_j, I)} = \frac{P(H_i|I)}{P(H_j|I)} B_{ij} \quad (5)$$

$P(d|I)$ is the normalization factor, and it cancels out giving:

$$B_{ij} = \frac{P(\vec{d}|H_i, I)}{P(\vec{d}|H_j, I)} \quad (6)$$

The equation above eqn(6) will be used to determine if a detected source is astrophysical (Veitch & Vecchio 2010).

1.7 Bayes Factors

To determine how effective of Bayesian analysis is as a low latency method for LIGO detections I will use two Bayes factors.

BSN is “the signal to noise coherent Bayes Factor” (Vajpeyi 2016). This Bayes factor is the probability that a detection is a signal given that noise is also occurring. Using the Bayesian theorem it is defined as:

$$P(S|N) = \frac{P(N|S) * P(S)}{P(N)} \quad (7)$$

As shown in (Vajpeyi 2016) this can be simplified to:

$$\log_{10}(BSN) = \log\left(\frac{s+n}{n}\right) \quad (8)$$

Where h is the probability of a detection being a signal and n is the probability of a detection being noise.

BCI is “The coherent versus incoherent log Bayes Factor” (Vajpeyi 2016). BCI is found from the BSN, particularly two different types of BSN. Both BSNs are defined the same, the difference is that the coherent Bayes factor is found from combining data from all detectors and the incoherent Bayes factor is found from only looking at one detectors components. BCI is defined as:

$$\log_{10}(BCI) = \log_{10}\left(\frac{BSN_{coherent}}{BSN_{incoherent1} + BSN_{incoherent2}}\right) \quad (9)$$

The Bayes factors are the primary parameters we will be using to find an efficient low latency filtering method for alerts.

1.8 Localizing Sources

Localization maps are created by using GW source parameters and antenna patterns of the LIGO detectors. When LIGO detectors detect a GW assuming it is astrophysical, the time delay between detections from different observatories can locate what direction the GW came from. The timing accuracy for a given source is:

$$\sigma_t = \frac{1}{2\pi\rho\sigma_f} \quad (10)$$

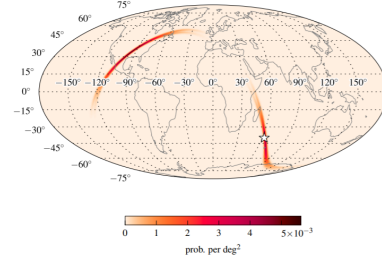


Figure 4. This is a skymap of a simulated gravitational wave source (Singer et al. 2014)

where ρ^4 and σ_f is the effective bandwidth. The localization will depend on the time delay as shown in:

$$p(r|R) = p(r) * e^{-\frac{(D \cdot (r-R))^2}{2(\sigma_1^2 + \sigma_2^2)}} \quad (11)$$

D is the distance between detectors, r is the reconstructed location, R is the position of the source and σ_1 and σ_2 are different σ_t values.

When localizing a source we find the smallest region of the sky that contains a source:

$$\frac{Area(.90)}{4} = 3.3 \frac{\sqrt{\sigma_1^2 + \sigma_2^2}}{D} \quad (12)$$

This gives the distribution of time observed with, t being the observed time, and T being the time of arrival at the sites. The result is a localization map as shown in fig(4).

Decreasing the size of the sky maps will result in faster multi-messenger counterpart searches.

1.9 Motivation

Comparing both Bayes Factors and *pastro*, we hope to find a reliable Bayes factor threshold from the comparison that will allow us to easily determine if an alert is astrophysical or not. We will do this by viewing Catalog(GWTC-2) and low latency(OPA) alerts (Prestegard 2021).

If our Bayes factor threshold allows us to more easily distinguish astrophysical alerts we will add these to the low latency packets. If the threshold yields no useful results, I will look into p-astro fig(2) to increase accuracy in a shorter amount of time.

An efficient low latency filtering method is valuable because it will allow us to conduct rapid multi-messenger counterpart searches upon receiving alerts(Chatterjee et al. 2020). Kilonovae are particularly interesting EM counterparts that will require a rapid EM follow up to observe. From BNS mergers heavy elements form that will decay radioactively which results in isotropic thermal expansion. The heavy elements are very neutron rich and this results in BNS mergers creating heavier radioactive elements than supernovae. The resulting energy will release bright emissions when the ejecta from the merger have spread out enough. These bright emissions can last for a few days (Metzger & Berger 2012). The

⁴ Signal to Noise Ratio

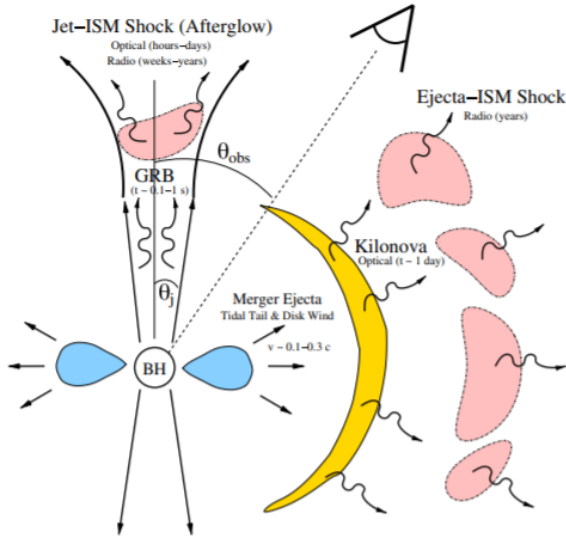


Figure 5. EM counterparts to BNS and NSBH mergers (Metzger & Berger 2012). In the figure you see the brief time we have to observe EM counterparts like kilonovae and afterglows. This is why an efficient low latency filtering method for LIGO alerts is so important.

name of such an event is a kilonova, represented by the yellow strain noise as a function of frequency in the detectors shown in fig(5). Kilonovae will require a rapid EM follow up due to their faintness, short lifespan, and prominence in IR, making detections difficult (Mohite et al. 2021). Observations from kilonovae will yield insights to many lingering questions within the astronomy community, such as Hubble constant adjustments, NS equation of state, and r-process nucleosynthesis.

2 OBTAINING AN THRESHOLD

2.1 Objective and approach

The goal of our project is to find a reliable low latency filtering method, in hopes that we can facilitate more rapid multi messenger counterpart searches upon receiving alerts.

To achieve this, we compare low latency and post processing Bayes factors and pastros from O3 alerts.

2.2 Obtaining Bayes factors and Pastros

We used the Gracedb database (Prestegard 2021) to access publicly released alert data. From the database we can extract the $\log_{10}(\text{BSN})$, $\log_{10}(\text{BCI})$ and pastros from Bayestar skymaps. We treat these as the low latency (OPA)⁵ data. In order to receive post processing bayes factors we ran Bayestar(Singer & Price 2016). For post processing pastros we used values from GSTLAL and PYCBC catalogs(GWTC-2)⁶ (Davis et al. 2021). We will treat all events from the catalogs(GWTC-2), GSTLAL and PYCBC as astrophysical,

⁵ OPA = Open Public Alerts

⁶ GWTC-2 = Gravitational Wave Transient Catalog -2

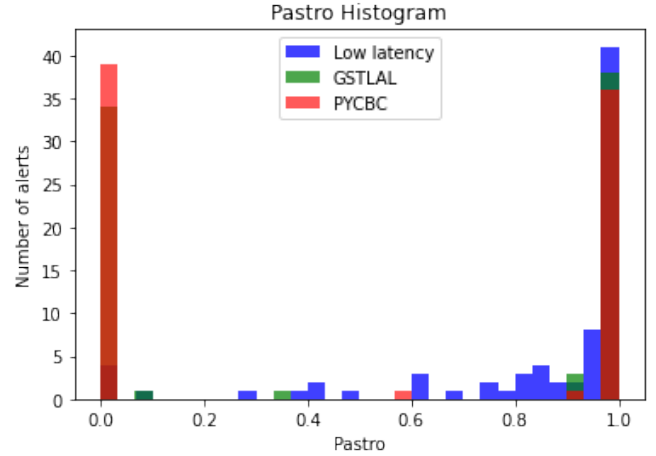


Figure 6. This figure shows the number of alerts vs. the pastro for low latency and catalog alerts. The three components have a total number of seventy-seven alerts. The image has bins = 30. There are 77 alerts in total for every pipeline and for low latency.

the events in low latency (OPA) that do not cross match with the catalogs are viewed as terrestrial.

There are 77 total alerts and 45 of those alerts are astrophysical.

2.3 Low latency vs. Post processing alerts

Before finding a threshold we should take a look at the difference between number of alerts at a certain pastro or $\log_{10}(\text{BCI})$ for GWTC-2 and OPA. Below, we also explain how each of these terms is defined.

To accurately compare the low latency and catalog values we crossmatched the events

Pastro is measured by comparing the differential rates of gravitational waves and background events (Lynch et al. 2018). Pastro has a minimum of zero and a maximum of one. If the pastro is zero the alert is very likely to be retracted; if pastro is equal to one it is likely to be an astrophysical alert.

There are two pipelines that are used for our analysis. GSTLAL is a pipeline that was primarily created for mergers of neutron stars and black holes, but also played an integral role in many other aspects of the LIGO collaboration (Canon et al. 2021). PYCBC is a pipeline that was created to meet the advanced detectors computational challenges (Dal Canton et al. 2014). There are different pastros derived from each pipeline’s independent analysis of astrophysical events that gets published in the catalog

When creating tables for the pastros of the two catalogs, if an alert was terrestrial the pastro is equal to zero, because it did not make it to the catalog. This explains the high density of pastro values equal to zero in fig(6). The figure also shows how polarized the two catalogs are. Most events are either equal to zero or 1, this fact will be more prevalent in later figures.

BCI is a Bayes factor derived from another Bayes factor eqn(9). The higher the value of this Bayes factor the more likely a candidate is to be astrophysical and the lower the value, the less likely it is to be astrophysical.

Running Bayestar required an alert to have made it to the

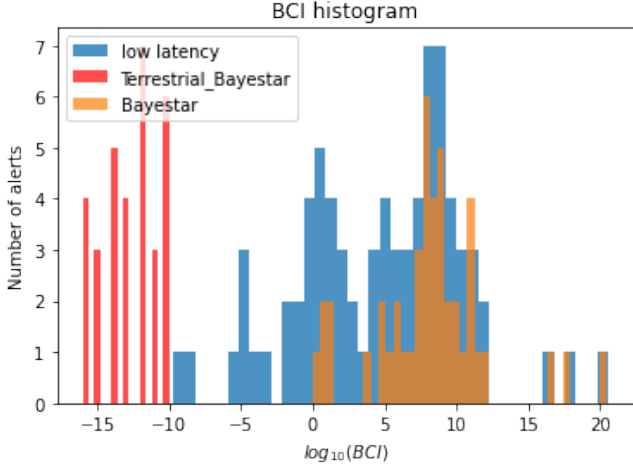


Figure 7. The Histogram is the Number of alerts vs. $\log_{10}(BCI)$. As previously stated, retracted events were given a random $\log_{10}(BCI)$ value between -10 and -15. The green bins are from low latency(OPA) and the blue bins are from Bayestar(GWTC-2). Both the green and blue bins have a total of 77 alerts. The number of bins = 40.

catalog. This caused a short-lived dilemma when trying to compare the updated BCI to the low latency BCI because we did not know what to set the terrestrial events equal to. Shreya Anand recommended setting the terrestrial alerts to an updated BCI that is less than -10. We gave the terrestrial values a random $\log_{10}(BCI)$ with a value between -10 and -15. This was done to avoid a polarized histogram as seen in fig(6) this way we may have a closer look at the values in between the two endpoints as shown in fig(7). fig(7) has a much better spread than fig(6), though the number of astrophysical Bayestar events stop around $\log_{10}(BCI) = 0$ leaving only retracted alerts below that value. This shows promise as it means a considerable number of terrestrial alerts are still left out of any threshold we set even if we include all astrophysical events.

2.4 Bayes factors vs. Pastro

The goal of our project is to see if using Bayesian factors is a reliable method for determining if a source is astrophysical or not. To determine if it is a reliable method, we plot two scatter plots, one scatter plot, plotting the low latency OPA Bayes factors and pastros and, the scatter plot on top of the previously mention plot, which plots the low latency pastro vs. the post processing Bayes factors.

The bayes factors used are all logarithmic, to achieve a more fair comparison to pastro we plot must plot pastro on a logarithmic scale.

Out of pure preference, we used terrestrial probability instead of pastro. Terrestrial probability is the probability that an alert is the result of terrestrial disturbance. To find the terrestrial probability we simple input:

$$p_{terr} = 1 - \text{pastro} \quad (13)$$

Plotting Terrestrial probability against $\log_{10}(BCI)$ yields the figure shown in fig(8). Looking at the scatter plots in fig(8),

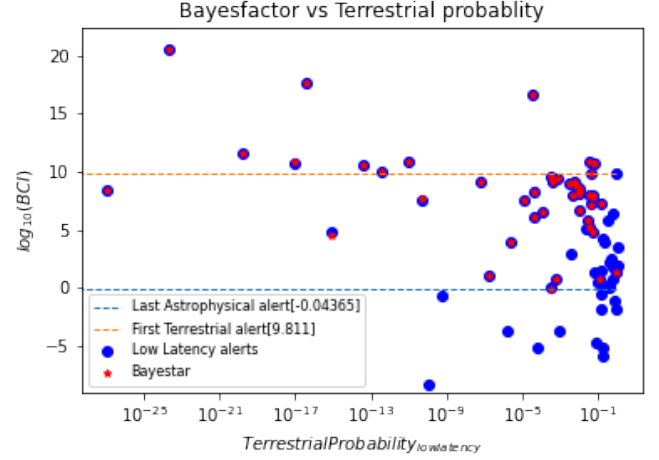


Figure 8. The figures above shows the $\log_{10}(BCI)$ (y-axis) vs. the probability of a detection occurring from terrestrial disturbance(x-axis). In the plot 'low latency alerts' are the blue circular points, it is a plot of low latency terrestrial probability vs $\log_{10}(BCI_{low-latency})$. Above the 'low latency alerts', we have 'Bayestar', these points are the low latency terrestrial probability vs the Bayes factors obtained from running Bayestar $\log_{10}(BCI)$, represented as a red star '*'. As in the previous section, the 'Bayestar' points below -10 $\log_{10}(BCI)$ are all terrestrial alerts. If a blue dot does not have the red star from Bayestar above it, that means that the alert is terrestrial as it did not make it to the catalog. There are 77 events in total

we can see that this method shows some promise in determining if sources are astrophysical or not. We can clearly see what value of $\log_{10}(BCI)$ yields the first terrestrial event and all astrophysical events. Fig(8) displays an issue when attempting to plot $\log_{10}(BCI)$ against terrestrial probability, most astrophysical alerts occur near Terrestrial probability = 0, but many retracted alerts do as well, making it difficult to comfortably set a threshold hold for pastro and terrestrial probability. The plot shows some promise in finding an BCI threshold, however further analysis between the fraction of alerts at a given threshold must be done.

The dotted red line in fig(8) allows us to view the $\log_{10}(BCI)$ value at which the first terrestrial alert occurs.

2.5 ROC curve

In order to find the optimal threshold for our Bayes factors and Pastro, we have to create an ROC curve. An ROC curve is the Receiver Operator Characteristic curve. It is made from a plot between the true positive rate(TPR) and false positive rate(FPR). ROC curves can tell us how well are data is at distinguishing the true and false results from each other, from this distinguishing, we can find a reliable and optimal threshold. If you create an ROC curve and the outcome is a diagonal slope from 0 to 1, your data is indistinguishable. However if your plots outcome is in the shape of a 90 degree angle, then your data is perfectly distinguishable (Sarang Narkhede 2021).

So first, we need to define the TPR and FPR.

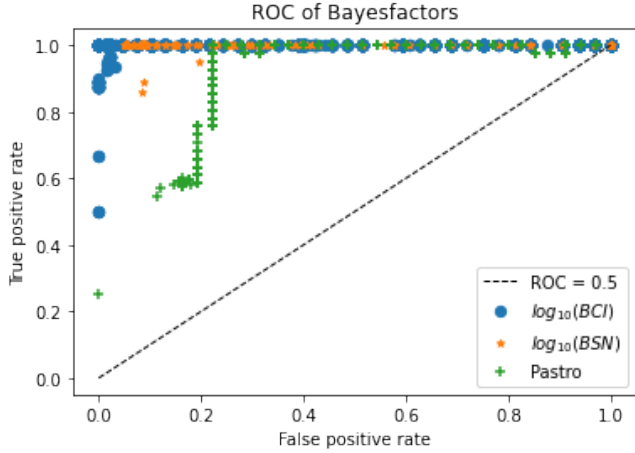


Figure 9. Plot of the ROC for $\log_{10}(\text{BCI})$, $\log_{10}(\text{BSN})$, and pastro . x-axis is false positive ratio and y-axis is the true positive ratio. The black dotted line, is a plot of where the TPR and the FPR are indistinguishable. Over 9000 thresholds were compared to create this plot. The blue dots represent $\log_{10}(\text{BCI})$, orange stars represents $\log_{10}(\text{BSN})$ and the green '+' represents pastro .

TPR is defined as:

$$\text{TPR} = \frac{\text{TP}}{\text{TP} + \text{FN}} \quad (14)$$

Where TP is the true positive⁷, FN is false negative⁸

FPR is defined as:

$$\text{FPR} = \frac{\text{FP}}{\text{FP} + \text{TN}} \quad (15)$$

Where FP is false positive⁹ and TN is true negative¹⁰ After these values has been found for a set of many thresholds, you can create your ROC curve by plotting TPR in the y-axis and FPR in the x-axis as shown in fig(9) The outcome of this plot is absolutely amazing! It shows that we have many choices for a reliable threshold for $\log_{10}(\text{BCI})$. There are also points on the plot for $\log_{10}(\text{BCI})$ where $\text{TPR} = 1$ and $\text{FPR} = 0$, signifying that there is a threshold that yields only astrophysical alerts!

Fig(9) proves that $\log_{10}(\text{BCI})$ is a very reliable statistic to find a threshold for because of the perfect 90 degree angle of its curve.

The next section will show us many of these thresholds and their reliability.

2.6 BCI threshold vs. Fraction of alerts

The best way to observe the validity of thresholds that we find with the ROC curve in fig(9) is to see how many astrophysical events out of the total astrophysical events are included at the different thresholds. Finding an comfortable balance between fraction of astrophysical alerts out of the total astrophysical alerts versus astrophysical alerts over total number of alerts

⁷ TP = Alerts are in both the catalog and OPA at threshold

⁸ FN = Alerts are not in OPA but in catalog at threshold

⁹ FP = In OPA but not in catalog

¹⁰ TN = Alert not in OPA and catalog

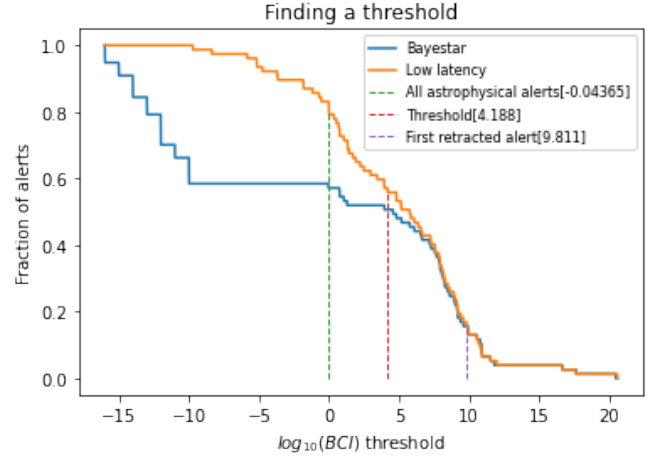


Figure 10. This plot can be used to find a reliable threshold. The x-axis consists of over 9000 $\log_{10}(\text{BCI})$ thresholds in the range of -15 to 21. The y-axis is the fraction of total alerts. The total number of alerts for 'Low latency' and 'Bayestar' is 77. As previously stated, for 'Bayestar' $\log_{10}(\text{BCI})_i = -10$ all events are retracted.

will be the deciding factor is our decision of a threshold. With fig(10), we can find such a balance. The three dotted lines in fig(10) represents three potential thresholds.

The purple dotted line marks the fraction of events passing the $\log(\text{BCI})$ threshold at which the first retracted alert occurs. This shows that at $\log_{10}(\text{BCI}) > 9.811$ you get a 100 percent of the events are astrophysical, however only 15 percent of the total alerts pass this threshold. Taking a closer look at the number of events, we see that there are 12 out of the 45 astrophysical alerts detected at this threshold, yielding a 26.7 percent fraction of total astrophysical events at this threshold.

The green dotted line represents the point where all astrophysical events are included in a threshold. At a threshold of $\log_{10}(\text{BCI}) < -0.04365$ you will have all 45 astrophysical alerts in your threshold, however at the exchange of a higher number of terrestrial events. At a threshold of -0.0435 you have 45 astrophysical alerts but a total number of 64 alerts, giving you a 70.3 percent of alerts total that are astrophysical.

We can use the two established thresholds as endpoints when selecting a threshold with a fair balance between terrestrial and astrophysical alerts.

The threshold we are looking for will be within the bounds of both endpoints as shown in eqn(16):

$$-0.0436 < \log_{10}(\text{BCI})_{\text{threshold}} < 9.811 \quad (16)$$

Where we are certain that there are 26.7 percent of total astrophysical events at $\log_{10}(\text{BCI}) > 9.811$

The red dotted line in fig(10) is what we found to be the threshold with the most favorable trade off between astrophysical and terrestrial alerts. When $\log_{10}(\text{BCI}) = 4.188$, we get 39 out of the total 45 astrophysical events, yielding 86.7 percent of all astrophysical events at this threshold. We get a total of 43 events at this threshold, dividing our 39 astrophysical alerts with the 43 total alerts detected at this threshold an astrophysical to total alert rate of 90.7 percent is found.

This result will allow us to be much more confident in

our low latency gravitational wave alerts. This in turn could potentially lead to a higher number of rapid multi messenger counterpart searches upon receiving alerts

3 CONCLUSION

Bayes factors have proven to be an extremely efficient method of filtering low latency LIGO alerts. Fig(9) shows that $\log_{10}(\text{BCI})$ is the best tool for distinguishing the right threshold, the plot confirms that $\log_{10}(\text{BCI})$ is better than both $\log_{10}(\text{BSN})$ and $\log_{10}(\text{pastro})$. Fig(10) provides a threshold boundary. If a low latency LIGO alert is obtained and its $\log_{10}(\text{BCI})$ value is within the boundaries stated, you now know the probability of that event being astrophysical. Furthermore any values above both boundaries can be interpreted as astrophysical. This result is major because it allows us to have near 100 percent confidence with low latency alerts.

Implementing these results in the process for filtering low latency results will prove to be advantageous. Testing the results obtained, with simulated events can provide evidence for the validity of our results.

If our final results prove to be effective in filtering out retracted events in the simulated events, we will implement it in the low latency packages.

The $\log(\text{BCI})$ threshold will allow rapid EM counterpart follow ups. The astronomer will be able to choose their own criteria for triggering a follow up as we can provide the probabilities of an alert being terrestrial for every $\log(\text{BCI})$ value.

4 ACKNOWLEDGEMENTS

I would like to thank everyone who collaborated with me for this project. Notably Shreya Anand, Alan Weinstein, LIGO Lab, Michael Coughlin, Leo Singer, Derek Davis, NSF, and Caltech for allowing me to participate in the program.

REFERENCES

- Callister T. A., Kanner J. B., Massinger T. J., Dhurandhar S., Weinstein A. J., 2017, *Classical and Quantum Gravity*, **34**, 155007
- Cannon K., et al., 2021, *SoftwareX*, **14**, 100680
- Chatterjee D., Ghosh S., Brady P. R., Kapadia S. J., Miller A. L., Nissanke S., Pannarale F., 2020, *ApJ*, **896**, 54
- Chen X., Shen Z.-F., 2019, arXiv e-prints, p. arXiv:1906.11055
- Dal Canton T., et al., 2014, *Phys. Rev. D*, **90**, 082004
- Davis D., et al., 2021, *Classical and Quantum Gravity*, **38**, 135014
- Kapadia S. J., et al., 2020, *Classical and Quantum Gravity*, **37**, 045007
- LIGO Scientific Collaboration V. C., 2021, Alert Contents, <https://emfollow.docs.ligo.org/userguide/content.html>
- LIGO Scientific Collaboration et al., 2015, *Classical and Quantum Gravity*, **32**, 074001
- Lynch R., Coughlin M., Vitale S., Stubbs C. W., Katsavounidis E., 2018, *ApJ*, **861**, L24
- Martynov D. V., et al., 2016, *Phys. Rev. D*, **93**, 112004
- Metzger B. D., Berger E., 2012, *ApJ*, **746**, 48
- Mohite S. R., et al., 2021, arXiv e-prints, p. arXiv:2107.07129
- Prestegard T., 2021, LIGO/Virgo O3 Public Alerts, <https://gracedb.ligo.org/superevents/public/03/>

- Sarang Narkhede N., 2021, ROC-AUC, <https://towardsdatascience.com/understanding-auc-roc-curve-68b2303cc9c5>
- Singer L. P., Price L. R., 2016, *Phys. Rev. D*, **93**, 024013
- Singer L. P., et al., 2014, *ApJ*, **795**, 105
- Vajpeyi S., 2016, Use of the Bayes Factor to Improve the Detection of Binary Black Hole Systems, https://dcc.ligo.org/public/0127/T1600254/001/AviVajpeyi_finalReport.pdf
- Veitch J., Vecchio A., 2010, *Phys. Rev. D*, **81**, 062003